Thermochimica Acta 482 (2009) 8–11

Contents lists available at ScienceDirect

Thermochimica Acta

journal homepage: www.elsevier.com/locate/tca

Study of temperature 3D profile during weld heating phase using Boubaker polynomials expansion

Salma Slama[a], Karem Boubaker[b,*,1], Jamel Bessrour[a], Mahmoud Bouhafs[a]

[a] UR Mécanique Appliquée, Ingénierie et Industrialisation (MA2I).ENIT, Tunisia
[b] E.S.S.T.T./63 Rue Sidi Jabeur 5100 Mahdia, Tunisia

ARTICLE INFO

Article history:
Received 19 June 2008
Received in revised form
13 September 2008
Accepted 25 September 2008
Available online 19 October 2008

PACS:
02.70.−c
07.05.Tp
44.05.+e
44.05.+e
82.20.Vj

Keywords:
Spot welding
Heat equation
Polynomial simulation
Temperature imaging
Boubaker polynomials expansion

ABSTRACT

The present study is concerned with investigating temperature evolution during weld heating phase in a particular device. Experimental results are presented as a guide to theoretical calculations. The main theoretical item is an attempt to solve the heat equation by considering the evolution of the source term inside electrically heated zone. Empirical variations of both thermal and electrical conductivities are treated and involved in the model.

1. Introduction

Several models of the resistance spot welding disposals and temperature profiling have been carried out these last decades. We can cite the works of Mohapatra et al. [1,2] who proposed models of thermal expansion in particular specimens, the simultaneous modulation model of Takegawa et al. [3] that monitored an efficient temperature modulation technique, the numerical model of Ding and Cheng [4] that yielded a differential scanning calorimetry protocol, and the model of Xu et al. [5] that developed a conjoint measurement of the temperature profile and the specific heat capacity using a low sample heat diffusivity and used *abacus* international code to develop a finite element model using coupled thermal–electrical–mechanical analysis.

Most of these studies were inspired by the theoretical study published by Morales [6] and that investigated temperature distributions in different materials.

In the last decade, the complete works of Srikunwong et al. [7–10] implemented a wide panoply of decoupled and coupled techniques to analyze heating and cooling processes mechanisms, which are associated with resistance spot welding. Their works used a recent finite element code: SYSWELD [11] in order to incorporate electrical–thermal and thermal–mechanical coupling procedures. They proposed realistic and efficient computational approach which took into account the temperature dependency characteristics and properties of both sheets and electrodes.

An other recent finite element code: ANSYS was recently use by Zhu et al. [12] who proceeded by updating parameter information in an incremental manner and realized accurate thermal–electrical–mechanical coupled numerical analyses.

The model we propose in this paper is inspired by these last few ones [7–10,12]. In fact, we intended to traduce the pulsed electrical supply into an incrementally incident source term and took into account electrical and thermal conductivities evolution at each

* Corresponding author.
E-mail address: managing_office069@yahoo.fr (K. Boubaker).
[1] Tutor.

0040-6031/$ – see front matter © 2008 Elsevier B.V. All rights reserved.
doi:10.1016/j.tca.2008.09.026

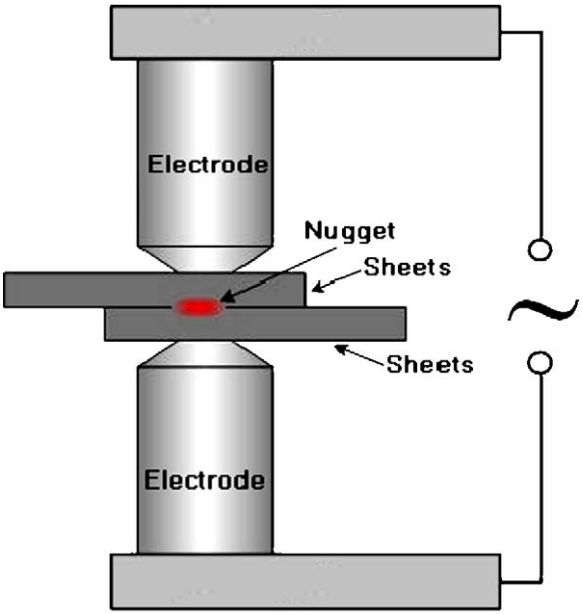

Fig. 1. Schematic diagram of the studied setup.

increment. The resulting temperature profiles have been discussed and successfully compared to similar results.

2. Model presentation

The studied device is presented in Fig. 1.

The weld operation is carried out by a combination of heat and pressure. The resistance of the sheets to current flow causes a localized heating in the central part. The pressure exerted by electrode extremities, through which the current flows, holds the opposite parts in intimate contact during the welding process. The duration of the operation is determined mainly by sheets thickness and type, the current intensity and the dimension of the electrodes. The material's transformation phases due to the velocity of cooling are not taken into account in this study.

The studied zone (nugget) geometrical features are presented in Fig. 2.

3. Theory

3.1. Coupled electrical–thermal heat equation

In the studied area described in Fig. 2, the coupled electrical–thermal heat equation traduces the energy balance in the central zone. This equation [13,14] is expressed by (1):

$$\begin{cases} \rho \times C \dfrac{\partial T(t,r)}{\partial t} = -\nabla q + P_e \\ q = -K \times \nabla T(t,r) \\ T(t,r) = T_r(r) \times T_t(t) \end{cases} \quad (1)$$

where ρ is the density, K the thermal conductivity, C the specific heat capacity, T the absolute temperature and P_e is the received electric power in one pulse.

By introducing the thermal diffusivity term: $D = K/\rho C$ and considering that the power current is modulated under the pulsation $\omega = 2\pi f$, this equation alters, in cylindrical coordinates to (2):

$$\left[\frac{\partial}{\partial r^2} + \frac{1}{r}\frac{\partial}{\partial r}\right] T_r(r) = \frac{j\omega}{D} T_r(r) + \frac{P_e}{K} \quad (2)$$

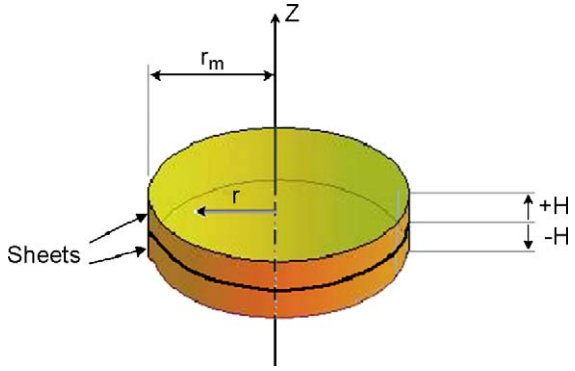

Fig. 2. Approximated schematic diagram of the nugget.

Table 1
Variations of electrical and thermal conductivities versus temperature.

Temperature (°C)	Electrical conductivity ($\Omega^{-1}\,m^{-1}$)	Thermal conductivity ($W\,m^{-1}\,K^{-1}$)
0	6000.2	52.3
200	4012.3	50.2
400	2014.5	48.0
600	1254.2	35.4
800	958.0	22.5
1000	954.8	28.2
1200	902.7	30.9
1400	857.9	34.8
1600	825.1	34.9
1800	802.3	35.7
2000	784.2	36.0

3.2. Solution using 4n-order Boubaker polynomials expansion

At this stage, T_r is expressed as an infinite expansion of the Boubaker polynomials [15–22]:

$$T_r(r) = \frac{T_0}{2N_0} \sum_{n=1}^{N_0} \xi_n B_{4n}\left(r\frac{\alpha_n}{r_m}\right) \quad (3)$$

where N_0 is a prefixed integer, α_n are the minimal positive roots of the Boubaker $4n$-order [15–17] polynomials B_{4n}, r_m is the maximum nugget radial range (Fig. 2) and ξ_n are coefficients to be found.

The Boubaker polynomials expansion has been used in many applied physics problems solutions [18–22]. The main characteristics of these polynomials and expansion are presented in Appendix A.

The derivation of the temperature expression is achieved by replacing the expression (3) in the main equation (2) and introducing initial conditions.

For a date which is an m-multiple of $\Delta t = 0.1$ s, the total received power is Eq. (4):

$$P_e\big|_m = \frac{1}{m\,\Delta t} \int_0^{m\,\Delta t} \left[\frac{2H}{\sigma_m S} \times I^2 t\right] dt \quad (4)$$

where H is sheet thickness and S is the heated subdomain section area. The indexed values of σ_m, the sheet–sheet global instantaneous electrical conductivity are obtained trough local polynomial regressions deduced from the given experimental values (Table 1).

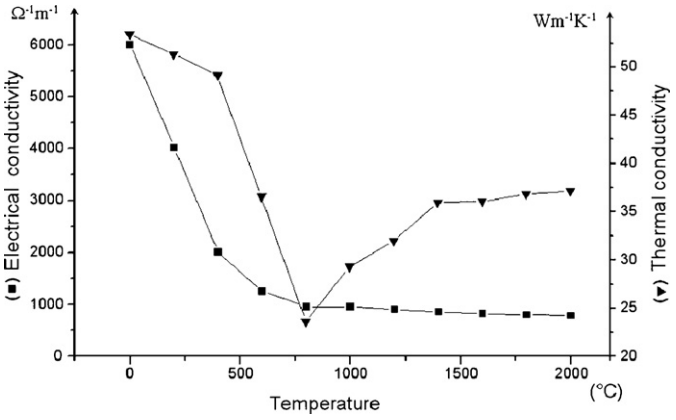

Fig. 3. Conjoint variations of thermal and electrical conductivities versus temperature.

By introduction of the expression (3) in the Eq. (2), we obtain Eq. (5)

$$\sum_{n=1}^{N_0}\xi_n \cdot \left[\left(\frac{\alpha_n}{r_m}\right)^2 B_{4n}''(\lambda\alpha_n) + \frac{\alpha_n}{r_m}\cdot B_{4n}'(\lambda\alpha_n) - \frac{j\omega}{D}B_{4n}(\lambda\alpha_n)\right] = 2N_0\frac{P_n}{K_m T_0}; \quad \lambda = \frac{r}{r_m} \tag{5}$$

where K_m is the temperature-dependent thermal conductivity. We can write (6):

$$\begin{cases} \sum_{n=1}^{N_0}\xi_n \Upsilon_n(\lambda) = 2N_0\dfrac{P_m}{K_m T_0} \\ \Upsilon_n = \left(\dfrac{\alpha_n}{r_m}\right)^2 B_{4n}''(\lambda\alpha_n) + \dfrac{\alpha_n}{r_m}B_{4n}'(\lambda\alpha_n) - \dfrac{j\omega}{D}B_{4n}(\lambda\alpha_n) \end{cases} \tag{6}$$

The indexed values of K_m are given by the empirical expression versus temperature, deduced from Table 1 and Fig. 3.

For resolution purposes, the relevant boundary conditions are gathered in Table 2.

Then, a uniform p-sampling is carried out along the r-axis (Fig. 2):

$$\begin{cases} \sum_{n=1}^{N_0}\xi_n \Upsilon_n(\lambda_p) = \sum_{n=1}^{N_0}\xi_n \psi_{n,p} = 2N_0\dfrac{P_m}{k_m T_0}; \quad \lambda_p = p\dfrac{r_m}{N_0}\Big|_{p=1\ldots N_0} \\ \psi_{n,p} = \Upsilon_n(\lambda_p) \end{cases} \tag{7}$$

This sampling leads to a matricial formulation (8):

$$[A]\times[\xi]_m = [B] \tag{8}$$

The system (8) is solved using Householder [23] algorithm applied to Petrov-Galerkin method [24–25].

Calculation details of the arrays $[A]$, $[\xi]_m$ and $[B]$ are presented in Appendix B.

The solution is obtained by introducing the calculated coefficients of the vector $[\xi]_m$ in the expression (3), the obtained temperature profile is presented in Fig. 4.

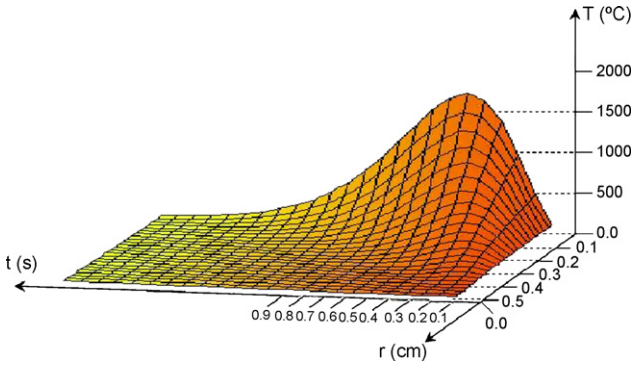

Fig. 4. 3D temperature profile.

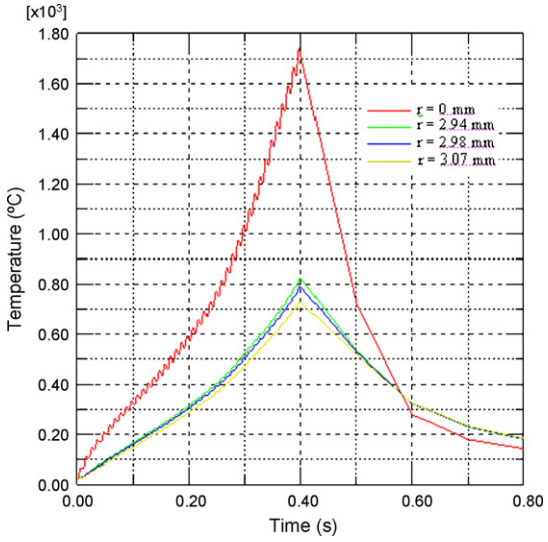

Fig. 5. Temperature variations versus time (precedent studies).

4. Discussion

The present theoretical profile (Fig. 4) is in concordance with the lastly [22] developed one (Fig. 5). In fact we can notice, i.e. that the location of the A_3 point location is approximately ($r(A_3)\approx 2.95$ mm). This distance is quite the same as in the temperature evolution yielded by a precedent study (Fig. 5).

The obtained temperature profile was also compared to the results yielded by Chuko and Gould [26] and Markiewicz et al. [27,28], some similarities were observed concerning the profile behaviour beneath the central heated zone. The maximal values were also concordant with the results published by Kolosov [29] and He et al. [30].

5. Conclusion

In the present paper, we tried to give a supply to recent works on temperature profiling inside special devices [1–7,24–29]. We tried

Table 2
Boundary conditions.

Boundary location	Temperature, T	Temperature first r-derivative: $\frac{\partial T(r,t)}{\partial r}$	Temperature second r-derivative: $\frac{\partial T(r,t)}{\partial r}$
$r=0$	T_0	0	0
$r=r_m$	T_∞	$\neq 0$	$\neq 0$

to introduce the variations of the relevant parameters incrementally, and hence solve the coupled electro-thermal balance equation at different t-dependent stages using the Boubaker polynomials expansion and some developed mathematical tools. The model is actually revised so that calculation allows taking into account the local pressure-induced constraints.

Appendix A

The Boubaker polynomials $B_n(X)$ have the following monomial definition:

$$\begin{cases} B_n(X) = \sum_{p=0}^{\xi(n)} \left[\frac{(n-4p)}{(n-p)} C_{n-p}^{p} \right] (-1)^p X^{n-2p} \\ \text{with :} \quad \xi(n) = \left\lfloor \frac{n}{2} \right\rfloor = \frac{2n + ((-1)^n - 1)}{4} \end{cases}$$

The symbol '$\lfloor\ \rfloor$' designates the floor function.

The Boubaker polynomials $B_n(X)$ have also the ordinary generating function:

$$f_B(X,T) = \frac{1+3t^2}{1-2Xt+t^2} \sum_{n=0}^{\infty} \tilde{B}_n(X) t^n$$

They are solutions to the homogenous differential equation:

$$(X^2-4)(3nX^2+4n-8)y'' + 3X(nX^2+12n-8)y' - n(3X^2n^2+4n^2-24n+32)y = 0$$

and verify Christoffel–Darboux-type formula:

$$\sum_{j=0}^{n} B_j^2 = \frac{B'_{n+1}(X) \times B_n(X) - B'_n(X) \times B_{n+1}(X)}{2}$$

The $4n$-Boubaker polynomials $\hat{B}_{4n}(X)$ are elements of a subset of the Boubaker polynomial sequence: they are defined by the explicit formula:

$$\hat{B}_{4n}(X) = 1 \times X^{4n} - 4(n-1)X^{4n-2} + \sum_{p=2}^{2n} \left[\frac{4(n-p)}{p!} \prod_{j=p+1}^{2p-1} (4q-j) \right] (-1)^p X^{2(2n-p)}$$

Many interesting proprieties of the $4q$-order Boubaker polynomials and their real roots were established and used. For example, when a function is expressed as an infinite sum of them as in Eq. (3), one can notice useful boundary conditions:

$$\begin{cases} \sum_{q=1}^{N} \xi_q B_{4q}(r) \Big|_{r=0} = 2N \neq 0; & \sum_{q=1}^{N} \xi_q \frac{\partial B_{4q}(r)}{\partial r} \Big|_{r=0} = 0 \\ \sum_{q=1}^{N} \xi_q B_{4q}(\alpha_q(r/R)) \Big|_{r=R} = \sum_{q=1}^{N} \xi_q B_{4q}(\alpha_q) \Big|_{r=R} = 0; & \sum_{q=1}^{N} \xi_q \frac{\partial B_{4q}(\alpha_q(r/R))}{\partial r} \Big|_{r=R} \neq 0 \end{cases}$$

Appendix B

In this appendix, the arrays of the system (8) are defined.

The system (8) is: $[A] \times [\xi]_m = [B]$ with

$$[A] = \begin{pmatrix} A_{1,1} & A_{1,2} & \cdots & \cdots \\ A_{2,1} & \cdots & \cdots & \cdots \\ \cdots & \cdots & \cdots & \cdots \\ \cdots & \cdots & \cdots & A_{N_0,N_0} \end{pmatrix}$$

where

$$A_{i,j} = \left(\frac{\alpha_i}{r_m} \right)^2 B''_{4i}(\lambda_j \alpha_i) + \frac{\alpha_n}{r_m} B'_{4i}(\lambda_j \alpha_n) - \frac{j\omega}{D} B_{4i}(\lambda_j \alpha_i)$$

Moreover,

$$[B] = \begin{pmatrix} b_1 \\ b_2 \\ b_3 \\ \cdots \\ \cdots \\ b_{N_0} \end{pmatrix}$$

where

$$b_j = N_0 \frac{P_j}{k_j T_0}$$

$[\xi]_m$ is the unknown vector which corresponds to the mth step: $[\xi]_m^{\mathrm{T}} = (\xi_1\ \xi_2\ \xi_3 \cdots \xi_{N_0})_m$

References

[1] G. Mohapatra, F. Sommer, E.J. Mittemeijer, Thermochim. Acta 453 (2007) 57–66.
[2] G. Mohapatra, F. Sommer, E.J. Mittemeijer, Thermochim. Acta 453 (2007) 31–41.
[3] K. Takegawa, K. Fukao, Y. Saruyama, Thermochim. Acta 432 (2005) 212–215.
[4] E.-Y. Ding, R.-S. Cheng, Thermochim. Acta 378 (2001) 51–68.
[5] S.X. Xu, Y. Li, Y.P. Feng, Thermochim. Acta 360 (2000) 131–140.
[6] J.J. Morales, Thermochim. Acta 178 (1991) 51–58.
[7] C. Srikunwong, T. Dupuy, Y. Bienvenu, Proceedings of the 7th International Seminar on the Numerical Analysis of Weldability, Graz-Seggau, 2003.
[8] C. Srikunwong, T. Dupuy, Y. Bienvenu, Scand. J. Metal. (2004).
[9] C. Srikunwong, "Sim. num. du procédé de soudage p. pts», Th. de Doct. de l'école des Mines de Paris, 2005.
[10] C. Srikunwong, T. Dupuy, Y. Bienvenu, Proceedings of the 15th Annual Conference of Mechanical Engineering Network of Thailand, vol. 2, Bangkok, Thailand, November, 2001, pp. 76–84.
[11] SYSWELD, Version 4.0, User's manual, ESI Group, 2000.
[12] W.F. Zhu, Z.Q. Lin, X.M. Lai, A.-H. Luo, Int. J. Adv. Manufact. Technol. 28 (1/2) (2006) 45–52.
[13] A. Chaouachi, K. Boubaker, M. Amlouk, H. Bouzouita, Eur. Phys. J. Appl. Phys. 37 (2007) 105–109.
[14] K. Boubaker, A. Chaouachi, J. Energy Heat Mass Transf. 29 (1) (2007) 13–25.
[15] H. Labiadh, K. Boubaker, J. Diff. Eq. Cont. Proc. 2 (2007) 117–133.
[16] H. Labiadh, M. Dada, K.B. Ben Mahmoud, A. Bannour, J. Diff. Eq. Cont. Proc. 1 (2008) 51–66.
[17] OTPDA, Les Polynômes de Boubaker, Dépôt légal no: 21-01-04-04-2007, Tunisia, 2007.
[18] K. Boubaker, Trends Appl. Sci. Res. 2 (2007) 540–544.
[19] J. Ghanouchi, H. Labiadh, K. Boubaker, Int. J. Heat Technol. 26 (1) (2008) 49–53.
[20] O.B. Awojoyogbe, K. Boubaker, Curr. Appl. Phys. 9 (2009) 278–283.
[21] K. Boubaker, Les Polynômes de Boubaker, Deuxièmes Journées Méditerranéennes de Mathématiques Appliquées JMMA02, Monastir, TUNISIE, March 2007.
[22] S. Slama, J. Bessrour, K. Boubaker, M. Bouhafs, COTUME 2008, 2008, pp. 79–80.
[23] M.W. Browne, J. Classif. 4 (2) (1987) 175–190.
[24] J. Sladek, V. Sladek, Ch. Zhang, M. Schanz, Comp. Mech., 37(3) (2006) 279–289.
[25] K.W. Morton, T. Murdoch, E. Süli, Numer. Math. 61 (1) (1992) 359–372.
[26] W.L. Chuko, J.E. Gould, Weld. J. 81 (2002) 1–6.
[27] E. Markiewicz, P. Ducrocq, P. Drazetic, G. Haugou, T. Fourmentraux, J.Y. Berard, Int. J. Mater. Prod. 16 (2001) 484–509.
[28] E. Markiewicz, P. Drazétic, Université de Valenciennes-Le Mont Houy, Mécanique et Industrie 4, 2003.
[29] V.I. Kolosov, Weld. Int. 9 (2) (1995) 151–152.
[30] X. He, T. Debroy, P.W. Fuerschbach, J. Appl. Phys. 94 (10) (2003) 6949–6958.